Virus Research 189 (2014) 214–225

Contents lists available at ScienceDirect

Virus Research

journal homepage: www.elsevier.com/locate/virusres

Genome-wide analyses of proliferation-important genes of Iridovirus-tiger frog virus by RNAi

Jun-Feng Xie[a,1], Yu-Xiong Lai[b,1], Li-Jie Huang[a], Run-Qing Huang[a], Shao-Wei Yang[a], Yan Shi[a], Shao-Ping Weng[a], Yong Zhang[a], Jian-Guo He[a,c,*]

[a] State Key Laboratory of Biocontrol/MOE Key Laboratory of Aquatic Product Safety, School of Life Sciences, Sun Yat-sen University, Guangzhou 510275, China
[b] Department of Nephrology, Guangdong General Hospital, Guangdong Academy of Medical Sciences, Guangzhou 518080, China
[c] School of Marine Sciences, Sun Yat-sen University, Guangzhou 510275, China

ARTICLE INFO

Article history:
Received 3 March 2014
Received in revised form 21 May 2014
Accepted 21 May 2014
Available online 2 June 2014

Keywords:
Iridovirus
Tiger frog virus
Genome-wide RNAi
siRNA
Essential gene

ABSTRACT

Tiger frog virus (TFV), a species of genus *Ranavirus* in the family *Iridoviridae*, is a nuclear cytoplasmic large DNA virus that infects aquatic vertebrates such as tiger frog (*Rana tigrina rugulosa*) and Chinese soft-shelled turtle (*Trionyx sinensis*). Based on the available genome sequences of TFV, the well-developed RNA interference (RNAi) technique, and the reliable cell line for infection model, we decided to analyze the functional importance of all predicted genes. Firstly, a relative quantitative cytopathogenic effect (Q-CPE) assay was established to monitor the viral proliferation in fish cells. Then, genome-wide RNAi screens of 95 small interference (si) RNAs against TFV were performed to characterize the functional importance of nearly all (95%) predicted TFV genes by Q-CPE scaling system. We identified 32 (33.7%) genes as essential, 50 (52.6%) genes as semi-essential and 13 (13.7%) genes as nonessential for TFV proliferation. Quantitative RT-PCR and titer assays of selected genes were performed to verify the screen results. Furthermore, the screened essential genes were analyzed for their genome distribution and conservative comparison within *Ranavirus*. Such a systematic screen for viral functional genes by cell phenotypes should provide further insights into understanding of the information in antiviral targets, and in viral replication and pathogenesis of iridovirus.

1. Introduction

Tiger frog virus (TFV), one kind of iridovirus, belongs to genus *Ranavirus* and it is the causative agent of a disease causing severe mortalities of commercial culture tiger frog tadpole (Weng et al., 2002), *Rana tigrina rugulosa*, and Chinese soft-shelled turtle, *Trionyx sinensis*, in China (unpublished data). TFV is a double-stranded DNA virus with large viral genome of approximate 105 kb. Analysis of the TFV genome sequence, which was available in 2002 (He et al., 2002), reveals that there are 104 predicted open reading frames (ORFs) in the genome and a number of conserved sequences which can be assigned a putative function based on homology in sequences (Iyer et al., 2001, 2006). TFV can infect a wide range of fish cell lines, for example fathead minnow (FHM) cells, carp *Epithelipma papillosum cyprinid* (EPC) cells and zebrafish embryonic fibroblast (ZF4) cells, with marked and typical lytic plaque forming cytopathogenic effects (CPE) (Luo et al., 2009; Weng et al., 2002). The severity of CPE in infected cells is relative to the proliferative condition of virus as well as viral quantity (Chinchar, 2002). Therefore, CPE observation can be an intuitive method to evaluate the proliferation of TFV. Since that TFV is highly homologous with frog virus 3 (FV3) which is the type species of genus *Ranavirus* (Chinchar et al., 2005), the study of TFV functional important gene screen by using loss-of-function technique, such as RNAi, will provide helpful information for ranavirus research.

RNA interference (RNAi) is a natural biological mechanism for silencing genes in most cells of many living organisms (Fire et al., 1998; Fjose et al., 2001). The potential therapeutic applications of the double-strand RNAs, particularly in preventing viral infections (Andino, 2003), are considerable for inhibition of essential gene, providing an efficient approach for systematic loss-of-function phenotypic analyses. Previous study of inhibition of TFV by small interfering RNA (siRNA) has built a successful platform for RNAi in fish cell line (Xie et al., 2005). Morpholino, another antisense technology recently developed, was also demonstrated to efficiently

* Corresponding author at: State Key Laboratory of Biocontrol/MOE Key Laboratory of Aquatic Product Safety, School of Life Sciences, Sun Yat-sen University, Guangzhou 510275, China. Tel.: +86 20 39332970; fax: +86 20 84113229.
E-mail addresses: lsshjg@mail.sysu.edu.cn, hillxjf@126.com (J.-G. He).
[1] These authors contributed equally to this work.

http://dx.doi.org/10.1016/j.virusres.2014.05.020
0168-1702/

block gene expression and proliferation of frog virus 3 (Sample et al., 2007). Therefore, the RNAi technique can be well applied to TFV-fish cell model. Genome-wide RNAi screens in yeast, *Caenorhabditis elegans* and Drosophila cells have demonstrated the potential of RNAi as a genomic tool to interrogate gene function (Ashrafi et al., 2003; Boutros et al., 2004; Fraser et al., 2000; Gönczy et al., 2000; Kamath et al., 2003; Lum et al., 2003). As for DNA virus, comparing to the eukaryotic genome containing a large number of genes, the relative small genome is feasible and also effective to perform genome-wide RNAi screen for important genes.

In the present study, we established a relative quantitative cytopathogenic effect (Q-CPE) assay of infected cells by detecting CPE emergence time and end-point CPE ratio to show the proliferation status of infectious TFV. Basing on the Q-CPE assay, we used RNAi to perform duplicate genome-wide analyses of functionally important TFV genes. Quantitative RTPCR and titer assays of selected TFV genes were performed to verify the screens. Genome distribution and conservative analyses with closely related ranaviruses were carried out for the screened important genes.

2. Materials and methods

2.1. Virus, cell and cell proliferation assay

For each sample of infection, TFV was freshly prepared from virus stock and the titer was determined by $TCID_{50}$ assay (Hamilton et al., 1977; Xie et al., 2005). Fathead minnow (FHM) cells were grown at 29 °C in M199 medium (Gibco, USA) supplemented with 10% fetal bovine serum (Gibco, USA), 100 U/ml penicillin, and 100 μg/ml streptomycin (Gibco, USA) in a 2.5% CO_2-humidified chamber. FHM cells amount in cytotoxicity assays of transfection were determined by The CellTiter 96® AQueous One Solution Cell Proliferation Assay (Promega, USA) according to the manufacturer's instructions.

2.2. Design and preparation of siRNA

Based on the transcript sequences of TFV, siRNAs targeting for 95 TFV ORFs (Table S1) were selected using Whitehead institute's online tool (http://sirna.wi.mit.edu/home.php) according to the principle as previously described (Elbashir et al., 2001; Schwarz et al., 2003; Xie et al., 2005). The previously determined non-transcribed ORFs, 013L, 060L, 070L, and 102R were excluded from RNAi assay (unpublished data). ORFs, 024R, 031L, 037L, 069R, and 086R were also omitted because their sequences are too small or too complex to design the ideal siRNAs for RNAi assay. Two irrelevant siRNAs (siIRT) without sequence similarity to any known gene were also designed as the first negative controls. All siRNAs including siIRTs were generated by In Vitro Transcription T7 Kits for siRNA Synthesis (Takara bio, Japan) and purified according to the manufacturer's protocol. The quality and concentration of purified siRNAs were assessed by gel electrophoreses and absorbance measurements. The concentrations of stocking siRNAs were diluted to 30 μM.

2.3. RNAi screen

In a 96-well plate, FHM cells at 2.5×10^5 were transfected with corresponding TFV-specific siRNA and irrelevant siRNA (the first negative control) at 500 nM using 0.8 μl of Lipofectamine 2000 (Invitrogen, USA) with quadruple replicates for each time interval. A sample of mock-transfection (MT) cells was established as the second negative control. Subsequently, three replicates were infected with TFV at multiplicity of infection (MOI=) 10. One well was left uninfected to serve as a negative control for the siRNA toxicity test. At 24, 36, 48, and 60 h post-infection (hpi), the cell status in the uninfected samples and the CPE in infected samples were examined. The culture supernatants of each siRNA were collected and combined for titer assay, and the cells were collected to extract total RNA for quantitative RT-PCR. The RNAi screening of FHM cells was performed twice.

To evaluate the inhibition efficiency and specificity of RNAi, nine TFV ORFs were selected for semi-quantitative RT-PCR (Sq-RTPCR) to detect the quantities of certain transcripts. After siRNA transfection and TFV infection, total RNAs from SB cells at 24, 36, 42, 48, and 60 hpi were extracted by Trizol (Invitrogen), treated with DNase I (Qiagen), and reverse transcribed by Superscript III (Invitrogen) to cDNAs. The produced cDNA was later used in Sq-RTPCR analyses with the 18S rRNA gene as the internal control. All RT-PCR amplifications were performed in the linear range. After electrophoresis, the gels were photographed, and images were analyzed by the ImageJ 1.37c software (NIH, USA). The pixel value (intensity) and area of each band in each image, as well as the background of a certain image, were measured. The average (AVG) and normalized AVG (nAVG) values to the internal control (18S) were generated as previously described (Xie et al., 2005). The nAVGs of samples from each detected ORF at five time intervals were normalized to the largest nAVG to generate the expression trend line (the expression rate in percentage). The expression ratios of each sample at five time intervals were averaged and intergroup comparisons were performed by Student's *t*-test. The primers used to amplify nine ORFs are shown in Table S4.

2.4. CPE observation and severity calculation

We developed a scaling system (i.e., Q-CPE assay) to characterize TFV proliferation by determining the CPE emergence time and severity of cell CPE at 60 hpi. The CPEs of the infected cells were analyzed and photographed under bright-field illumination using a Nikon Eclipse TE-2000U microscope at 24, 36, 48, and 60 hpi. Five fix-fields (up, down, left, right, and central field without overlap) of each well were photographed. These four time intervals were set as observation and sampling points. The CPE emergence time was determined by the first time interval when CPEs of cell enlargement, detachment, or viral plaques formation were identified. The viral plaques in the photos of each sample at 60 hpi were manually selected and the CPE cell ratio of (plaques area)/(total area) was calculated by Image-Pro PLUS V5.1.0.20 (Media Cybernetics, Inc., USA). Score A is the parameter for CPE emergence time and each time interval was assigned as follows: 0.04 for 24 hpi, 0.08 for 36 hpi, 0.24 for 48 hpi and 0.75 for 60 hpi. Score A is derived from the CPE cell ratios of TFV-infected MT samples. Early CPE emergence led to low scores. Score B is the parameter for CPE severity at 60 hpi and was obtained by calculating the CPE cell ratio with the following formula: score B = 1 − (plaques area/total area). For each sample, a final *z* score was obtained by adding up scores A and B. The *z* score can be used to evaluate TFV proliferation under normal or RNAi conditions.

2.5. Quantitative RT-PCR assay

Real-time quantitative RT-PCR (Q-RTPCR) method was used to measure mRNA copies of TFV *mcp* (major capsid protein) gene (He et al., 2002) which is a valuable detection marker for ranavirus infection (Tidona et al., 1998). Total RNAs of infected cell samples were isolated (Trizol, Invitrogen), DNase I treated (Qiagen) and reverse transcribed (Superscript III, Invitrogen) to cDNAs which were later applied to quantitative PCR analyses with Taqman MGB (Minor Groove Binder) probe method according to previously described (Wu et al., 2007). 18S rRNA of FHM cell was used as internal control. Two sets of primers used in the assay are *mcp* set (T096Q-Forward: 5′-TTATGGTGCAGAACGTCACACA-3′,

T096Q-Reverse: 5′-CGGGAGTGACGCAGGTGTA-3′) with green fluorescent FAM (6-carboxy-fluorescein) labeled probe (T096Q-Probe: 5′-FAM-TTCCGTCGGCTCC-MGB-3′) and 18s rRNA set (18SQ-Forward: 5′-ACGCTATTGGAGCTGGAATTACC-3′, 18SQ-Reverse: 5′-GGCGAGGAC CCATTGGA-3′) with red fluorescent VIC (fluorescein derivate) labeled probe (18SQ-Probe: 5′-VIC-CACCAGACTTGCC-MGB-3′). Statistical analyses of normalization for two channels of fluorescence signals were performed using ABI Prism 7000 Sequence Detection System Software (SD1.0) and the expression ratios of all samples were generated (Liu and Saint, 2002). All quantitative RT-PCR assays were repeated for three times. The averages of four time-intervals expression ratios of each sample were analyzed and grouped by hierarchical clustering (Cluster 3.0). Intergroup comparisons were performed by a Student's *t* test.

2.6. Titer assay

TFV titer assay, which is a traditional virulent assay of infectious virus, was performed using the supernatants of samples of indicated time-intervals as previously described (Xie et al., 2005; Weng et al., 2002). Briefly, viral supernatants of different time-intervals were diluted from 10^{-1} to 10^{-8} and used to infect FHM cells with 6 repetitions per dilution to perform $TCID_{50}$ assay. $TCID_{50}$ of each sample was calculated as described by Reed–Muench (Reed and Muench, 1938) and Spearman–Karber method (Hamilton et al., 1977). The averages of four time-intervals titers of each sample were analyzed and grouped by hierarchical clustering (Cluster 3.0). Intergroup comparisons were performed by a Student's *t* test.

2.7. Computational analysis of RNAi results

To identify conditions with siRNA-specific repression of TFV proliferation, data of duplicate screens were averaged. Correlation coefficient calculation of *z* scores from two screens were calculated and showed that nearly identical results were obtained in two screens. The data from samples of MT and two siIRTs were named control sets and a baseline was generated from the mean of *z* score of all negative controls. We set a *z* score superior threshold of three folds more than the baseline to select the TFV proliferation essential genes (EG) (Boutros et al., 2004). Another threshold, an inferior threshold which is of three standard deviations from the baseline was also set and the average *z* scores of TFV genes below this threshold indicate are classified as non-essential gene (NEG) to viral proliferation. While the *z* scores between these two thresholds means the genes are semi-essential (SEG) to viral proliferation. For the most statistically significant selection of average *z* scores, we set a threshold of one standard deviation of all samples from the mean or above to choose "the most important EG (mEG)".

Nucleotide and amino acid sequences were analyzed using the DNASTAR software package (Lasergene, Madison, WI, USA). Nucleotide sequence and protein database searches were performed using the BLAST programs at the NCBI website http://www.ncbi.nlm.nih.gov. The predicted protein sequences of genes identified by RNAi phenotypes were searched for conserved protein domains using online programs including http://smart.embl-heidelberg.de and http://www.ncbi.nlm.nih.gov/Structure/cdd/wrpsb.cgi.

3. Results and discussion

3.1. A scaling system for screening functional important TFV gene by RNAi

Vertebrate iridoviruses, specifically members of the genus *Ranavirus*, have become significant causes of diseases in ectothermic animals. Such viruses have been the subject of research with a long history and deserve further study from virological, commercial, and ecological points of view (Chinchar, 2002). TFV belongs to the genus *Ranavirus* in family *Iridoviridae*, and the type species of this genus is frog virus 3 (FV3) which is most closely related to TFV in genomic sequence (Tan et al., 2004). TFV shares high homologue with FV3 and they may represent strains of the same viral species (Chinchar et al., 2005). Therefore, we can integrate the available information on FV3 and RNAi to elucidate the relationship between TFV ORFs involved in viral replication and infection.

To monitor the proliferation level and quantity of TFV in the infected cells, we developed a quantitative method based on CPEs of infected cells under RNAi conditions in two aspects: the CPE emergence time and CPE severity at a certain period post-infection. The scaling system, Q-CPE, was used to characterize the importance of a gene to TFV proliferation based on a significance factor, the *z* score, which represents the severity or rank of specific RNAi cell CPE phenotypes. A *z* score is composed of two parts was used to precisely reflect the phenotype. Score A originated from CPE emergence time, and score B originated from CPE severity at 60 hpi. The calculation of scores A and B was mentioned in Materials and methods. Fig. 1A shows the well stability and repeatability of TFV infection at MOI = 10 to generate CPE on FHM cells. With this scaling system, we can screen TFV ORFs and rank their importance for viral proliferation. Thus, the CPE emergence time represents the viral quantity caused by the first several rounds of viral proliferation. The silencing of a functionally important viral gene hampers or blocks viral proliferation and postpones or inhibits CPE emergence. The severity of CPE at a later time point of infection, such as 60 hpi, represents the viral accumulation that is proportional to severity. Therefore, the visible cell phenotypic changes at 60 hpi not only indicate the viral quantity but also increase the low quantitative differences of early infection to a distinguishable level by the quantities of viral plaques. Due to the complicated connection of viral gene expression, a certain gene silenced by RNAi is likely to hamper the replication cycle resulting in the following: (i) delay of CPE emergence and no severity CPE at 60 hpi because of the presence of an essential gene for propagation, (ii) no delay of CPE emergence but no severity CPE at 60 hpi, (iii) no delay of CPE emergence but no CPE aggravation thereafter, or (iv) no delay of CPE emergence and severity CPE at 60 hpi as the negative control. Accordingly, CPE emergence time and CPE severity at 60 hpi should be evaluated to quantitatively determine the significance of viral genes. The *z* score as a significant index generated by Q-CPE can reflect the importance of screened genes. In a word, the more important the functional gene needs for TFV proliferation in RNAi condition, the later CPE emerges and the slighter CPE severity appears at 60 hpi. However, the CPE emergence time (score A) and severity at 60 hpi (score B) can be estimated separately by comparing the behavior of genes in detail.

Q-CPE assay was selected because it includes the morphology of viral plaques at certain infection time points and the emergence time. When a single parameter is used, Q-CPE assay is more informative, valuable, and precise than other assays, such as MTT (Crouch et al., 1993; Petty et al., 1995) and plaque reduction (Hsuana et al., 2009; Serkedjieva and Ivancheva, 1999). MTT assay detects cell viability, whereas plaque reduction assay measures plaque formation at a single time point. The results of MTT assay are sometimes inconsistent with those of plaque reduction assay, particularly when determining antiviral effects (Liu et al., 2005). By contrast, Q-CPE can be used to directly observe CPEs at multiple endpoints without adding any reagents to infected cells.

Furthermore, the transfection reagent used in the screening procedure is non-toxic to FHM cells at a working concentration of 0.8 μl per well (Fig. 1B) determined by cell proliferation assay. The concentration of siRNA is important to ensure the accuracy of RNAi

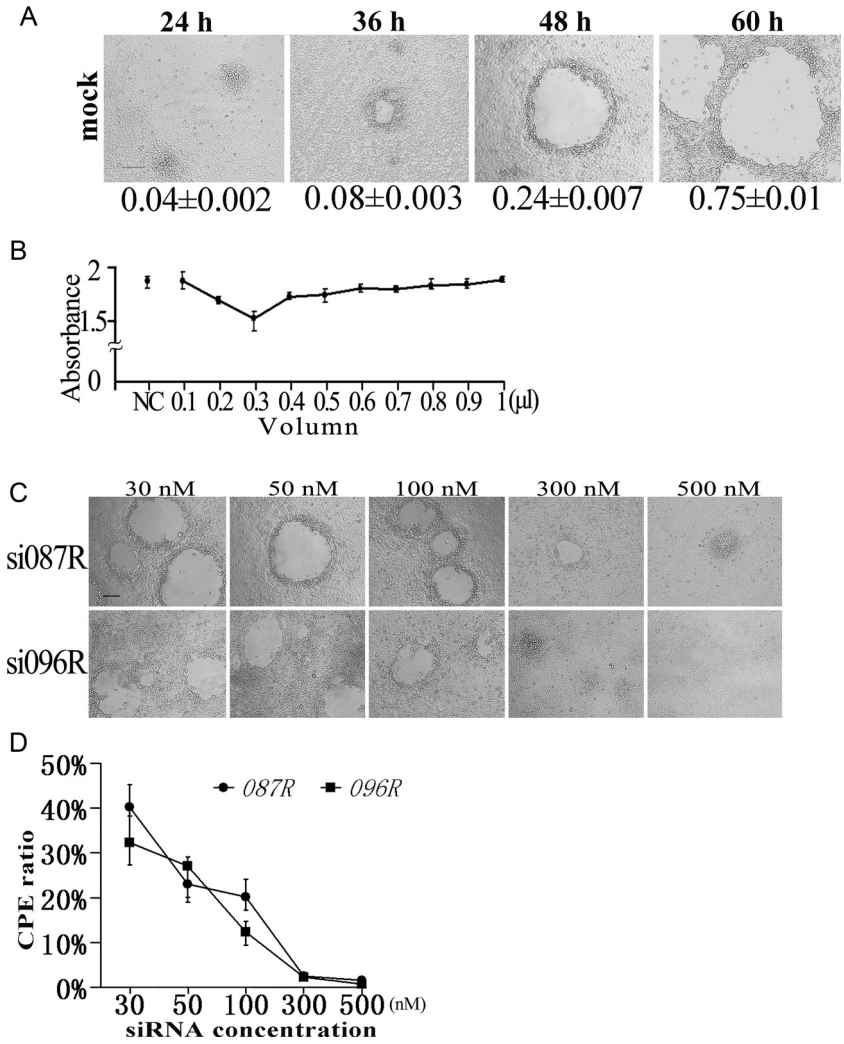

Fig. 1. Development of quantitative cytopathogenic effect assay system. (A) CPE of FHM-TFV infection model at different time points. FHM cells were infected with TFV and the ratio of plaques area/total area were obtained at 24, 36, 48, and 60 hpi with standard deviation as indicated in the figures. (B) Effect of transfection reagent to FHM cells viability. FHM cells were treated with different volumes of Lipofectamine 2000 as indicated and cell viability was determined by CellTiter 96® AQueous One Solution Cell Proliferation Assay. The optimal quantity of 0.8 μl per well was set as working concentration. (C) Determination of siRNA's concentration. Two siRNAs, si087 and si096, were transfected into FHM cells in different concentrations as indicated before TFV infection. The CPE of 60 hpi were shown and the RNAi effect is dose-dependent. (D) Determination of siRNA's concentration. The CPE ratio of each sample was calculated and the line graph was generated. The best siRNA working concentration is 500 nM. Independent assays were repeated at least three times. The average data are shown and the error bars indicate standard deviation.

assay. We examined the CPE assay ratios of the cells (Fig. 1C) transfected with different concentrations of 087R- (immediate early gene) and 096R- (late gene) specific siRNAs that were set as positive controls. Results show that the RNAi effect to TFV at 60 hpi is dose dependent and that the best working concentration of siRNA is 500 nM (Fig. 1D). The dose-dependent effect of RNAi are normally observed in viral silencing (Abdulnaser et al., 2009; van den Born et al., 2005), suggesting that the inhibition of viral replication significantly varies depending on the target gene. Nevertheless, the usage of 500 nM siRNA is theoretically sufficient to inhibit viral genes in RNAi experiment.

3.2. Genome-wide RNAi analyses of TFV proliferation-important genes

Combining the well-developed RNAi strategies in fish cells (Xie et al., 2005), we performed the genome-wide RNAi against TFV. Genome-wide and high-throughput RNAi is widely used in screening for different purposes (Bettencourt-Dias et al., 2004; Boutros et al., 2004; Fraser et al., 2000; Gönczy et al., 2000; Kamath et al., 2003; Maeda et al., 2001). This technology is efficient for systematic loss-of-function phenotypic analyses (Lum et al., 2003; Ramet et al., 2002). RNAi has been applied to determine viral genes that are essential for viral replication and the approach has also been applied to identify potential chemotherapy targets, design viral vectors, and generate attenuated vaccines (Brune et al., 1999).

To classify the functionally important genes of TFV, ninety-five TFV transcripts within ORFs were specifically inhibited by siRNA-mediated RNAi to accomplish the genome-wide primary screen. The screening was performed twice and a comparison between duplicate screens revealed highly qualitatively and quantitatively reproducible results (Fig. 2A) with a correlation coefficient of 0.99, indicating that the reproducible RNAi results can be quantified by *z* score. The *z* score also represents the severity or rank of specific RNAi phenotypes. The complete data set is shown in Table 1 and Table S2. The average *z* score of the all controls, namely the baseline, is 0.28. To identify the EGs for TFV proliferation, a superior threshold of *z* score of 0.85 is set, representing that the *z* scores of EGs are three-fold more than the baseline. By contrast, an inferior threshold for NEG was also set as a *z* score of less than 0.3, which was

Table 1
TFV ORFs and the results of RNAi screens.

ORF[a]	No. of amino acid	Predicted structure or function	CPE emergence time (hpi)[b]	Pixels at 60 hpi[c]	The *z* score[d]	Group[e]
001L	338	Envelope protein	60	41,203	1.718	EG
003L	70		24	425,208	0.714	SEG
004R	404		24	445,688	0.699	SEG
005R	60		24	944,432	0.317	SEG
006R	200		24	566,316	0.606	SEG
007L	142		24	522,105	0.640	SEG
008R	1294	DNA-dependent RNA polymerase I (DdRP I) largest subunit-like protein	24	914,411	0.340	SEG
009L	948	Helicase	48	464,877	0.884	EG
010R	137		60	15,053	1.738	EG
011R	70		24	949,659	0.313	SEG
012L	297		36	226,956	0.906	EG
014L	50		24	1,011,102	0.266	NEG
015R	119		36	23,881	1.062	EG
016R	315	ABC_ATPase (Poxvirus A32 protein)	24	541,563	0.625	SEG
017R	275	Integrase	24	994,332	0.279	NEG
018L	502		24	879,427	0.367	SEG
019R	931		24	931,107	0.327	SEG
020R	152	Envelope protein	60	14,623	1.739	EG
021L	219		24	895,358	0.354	SEG
022R	975	D5 family ATPase	36	41,418	1.048	EG
023R	382		60	9754	1.743	EG
025R	259	p31K-like protein	60	20,911	1.734	EG
026R	52		24	994,814	0.278	NEG
027R	259	eIF-2α-like protein	24	865,469	0.377	SEG
028L	62		24	888,368	0.360	SEG
029R	970	Tyrosine protein kinase/putative lipopolysaccharide-modifying enzyme	48	224,236	1.068	EG
030R	162		36	817,419	0.454	SEG
032R	139		24	897,150	0.353	SEG
033R	649	Neurofilament triplet H1-like protein (NTH1)	24	704,675	0.500	SEG
034R	63		24	871,274	0.373	SEG
035L	47		36	721,583	0.528	SEG
036R	132		60	17,197	1.737	EG
038L	131		60	36,282	1.722	EG
039R	44		24	1,006,931	0.269	NEG
040R	218	Catalytic domain of ctd-like phosphatase	36	657,840	0.576	SEG
041R	565	Ribonucleoside-diphosphate reductase α (RDRA) chain	60	61,065	1.703	EG
042R	116	Hydrolase of the metallo-β-lactamase superfamily	24	828,697	0.406	SEG
043R	182		24	911,929	0.342	SEG
044R	88		24	859,193	0.382	SEG
045R	1165		60	14,965	1.739	EG
046L	409		36	925,293	0.372	SEG
047L	136		24	991,872	0.281	NEG
048L	152	Neurofilament triplet H1-like protein (NTH1)	60	14,445	1.739	EG
049L	138		24	1,004,647	0.271	NEG
050L	83		36	356,665	0.807	SEG
051L	194	SAP DNA-binding protein	60	26,932	1.729	EG
052L	246		36	971,085	0.337	SEG
053R	561		24	359,802	0.765	SEG
054L	355	3β-hydroxy-Δ5-C27-steroid oxidoreductase (3β-HSD)	24	956,640	0.308	SEG
055R	522	Myristylated membrane protein	24	897,603	0.353	SEG
056L	431	Helicase-like protein	24	999,732	0.275	NEG
057L	49		24	355,096	0.768	SEG
058R	134		24	954,825	0.309	SEG
059R	498	Phosphotransferase	36	946,157	0.356	SEG
061R	184		24	984,727	0.286	NEG
062L	352		36	634,160	0.594	SEG
063R	1013	DNA-dependent DNA polymerase (DdDP)	24	885,125	0.362	SEG
064R	40		24	942,067	0.319	SEG
065L	1219	DNA-directed RNA polymerase II (DdRPII) second largest subunit	36	44,187	1.046	EG
066L	52		36	748,467	0.507	SEG
067L	42		36	816,452	0.455	SEG
068R	164	Deoxyuridine triphosphatase (dUTPase)	24	990,806	0.281	NEG
071L	387	Ribonucleoside-diphosphate reductase β chain (RDRB)	24	855,109	0.385	SEG
072R	65		60	49,750	1.712	EG
073L	51		36	64,930	1.030	EG
074R	88		36	299,838	0.850	EG
075R	131		48	33,946	1.214	EG
076R	77		24	87,297	0.973	EG
077L	238		60	26,832	1.729	EG
078L	324	NTPase/helicase-like protein	24	895,214	0.355	SEG
079L	330		24	815,392	0.416	SEG
080L	84	Possible membrane-associated motif in LPS-induced tumor necrosis factor α factor (LITAF)	24	934,721	0.324	SEG

Table 1 (*Continued*)

ORF[a]	No. of amino acid	Predicted structure or function	CPE emergence time (hpi)[b]	Pixels at 60 hpi[c]	The *z* score[d]	Group[e]
081R	73		48	30,253	1.217	EG
082L	115		36	989,016	0.323	SEG
083L	224		36	995,420	0.318	SEG
084R	572	ATPase-dependent protease/AT_hook domain	24	84,206	0.976	EG
085L	371	Ribonuclease III (RNase III)	36	956,020	0.348	SEG
087R	157	Immediate early protein (ICP-18)	36	14,841	1.739	EG
088R	124	Thymidylate synthase (TS)	48	94,963	1.167	EG
089R	214	Cytosine DNA methyltransferase (DMet)	48	209,101	1.080	EG
090R	245	Proliferating cell nuclear antigen (PCNA)	24	997,970	0.276	NEG
091R	195	Thymidine kinase (TK)	36	997,463	0.316	SEG
092L	97		24	944,584	0.317	SEG
093L	605		24	545,612	0.622	SEG
094R	150	Thiol oxidoreductase	24	875,215	0.370	SEG
095R	398		24	999,675	0.275	NEG
096R	463	Major capsid protein (MCP)	36	15,541	1.228	EG
097R	395	Immediate early protein (ICP-46)	60	21,919	1.733	EG
098R	101		36	984,909	0.326	SEG
099L	55		24	505,459	0.653	SEG
100L	155		24	419,287	0.719	SEG
101R	390	DNA repair protein RAD2	48	76,561	1.181	EG
103R	223		24	972,041	0.296	NEG
104R	149	Myeloid cell leukemia protein (MCL)	60	20,632	1.734	EG
105R	256	Replicating factor (RF)	24	1,016,471	0.262	NEG
MT			24	1,006,327	0.270	
siIRT1			24	975,916	0.293	
siIRT2			24	982,364	0.288	

[a] ORF numbering and putative function are updated from previous studies (Eaton et al., 2007; He et al., 2002; Wang et al., 2008) and unpublished data; L and R represent the orientation of ORF. The negative control sets were composed of mock-transfection (MT) and two irrelevant siRNAs (siIRT1/2) transfected samples.

[b] A fix digit (score A) was assigned to each time-interval of CPE emergence, 0.04 for 24 hpi, 0.08 for 36 hpi, 0.24 for 48 hpi and 0.75 for 60 hpi, respectively.

[c] Cell CPE at 60 hpi of all samples were checked. Five fix-fields of each well were photographed, the viral plaques in the photos were manually selected and plaques areas were calculated by image software. Score B of each sample was calculated by formula: score B = 1 − (plaques area/total area). The average pixels from two screens were shown.

[d] The *z* score = score A + score B. The average *z* score from two screens were shown.

[e] TFV ORFs were divided into EGs, SEGs and NEGs by two thresholds, 0.85 and 0.3. The ORF which *z* score was larger than 0.85 was designated as EG, while ORF with *z* score lower than 0.3 was assigned to NEG. The ORF with *z* score between 0.85 and 0.3 was grouped as SEG.

one standard deviation from the mean of all control samples (baseline). The genes with *z* score between these two thresholds were defined as SEG in viral proliferation. Of the 95 investigated genes, 32 were assigned as EG, 50 as SEG, and 13 as NEG for TFV proliferation based on the scaling system (Table 1). The ratios of EG, SEG, and NEG were 33.7%, 52.6%, and 13.7%, respectively (Fig. 2B). In terms of the half inhibition efficiency, which means 48 of all screened genes should be silenced, the median sample of ranked genes by *z* score, ORF033R (*z* score = 0.5), was statistically distinguishable from that of the control sets ($p < 0.01$, Table 1). This result implies that the RNAi screens are reliable. A limitation of RNAi screening may be homology constraints in primer design for the generation of dsRNAs that target very closely related genes. As evident from these tests, cross-match sequence identity to off-target genes is not a major problem in identifying specific phenotypic results. However, there is a risk of silencing a certain ORF with only one siRNA, because the silencing efficiencies might be unsteady and lead to false negative results, implying that two or three siRNAs should be used to target a specific ORF (Sample et al., 2007; Xie et al., 2005). Nevertheless, the genome-wide screening of TFV EGs using RNAi as a screening platform can provide a thorough understanding of viral genes connection and their comparative importance by quantity, and provide clearer quantitative comparison results than single gene silencing (Kim et al., 2010; Whitley et al., 2010) or multiple gene inhibition (Sample et al., 2007; Whitley et al., 2011).

To determine the RNAi efficiency, we performed Sq-RTPCR assay to evaluate the quantity variation of transcripts of certain ORFs. Nine ORFs, including 001L, 087R, and 097R from EG, and 009L, 016R, 022R, 078L, 089R, and 101R from SEG, were selected for Sq-RTPCR after TFV infection. The Sq-RTPCR results are shown in Fig. S1 and Fig. 3. As shown in Fig. 3, the expressions of all nine ORFs were inhibited by the corresponding siRNA at five time intervals and all the average expression rates to MT samples were less than 50% (from 3% to 45%). This result indicates the efficient silencing effect on the screens. Moreover, these nine ORFs represent the three temporal categories of TFV expressing ORFs, including immediate early (IE) gene (ORFs 087R and 097R), delay-early (DE) gene (ORFs 009L, 016R, 022R, 078L, and 089R), and late (L) gene (ORFs 001L and 101R). The inhibition efficiency of the IE genes was significant ($p < 0.05$) under RNAi conditions. However, the comparison of IE gene expression under MT and no treatment (NT) conditions showed that the outside stimulation, namely liposome stimulation in MT, may affect the normal expression of the IE genes. The strong regulatory effect of the IE genes may be responsible for the active reaction (expression variation) to external stimuli, such as liposome. Therefore, the data of MT samples were used as standards to normalize the expression rate. The DE and L genes were different from the IE genes because their expression levels were similar in MT and NT samples. The L genes, ORF001L and ORF101R, were affected less by liposome stimulation than the DE genes. Nevertheless, the expression level of ORF001L or ORF101R did not significantly change under the MT and siRNA-transfected conditions at five time intervals. The L genes maintained low expression levels during the early stage (before 48 hpi) with minimal difference from the MT samples and were mainly expressed in the late stage (after 48 hpi). Accordingly, the notable silencing effect in the late stage failed to generate an overall significant difference at all time intervals. However, the silencing effects of si001 and si101 were high and clearly shown by the average expression rates of ORF001L (11%) and ORF101R (3%).

In the genome-wide RNAi analysis, an uninfected control of each siRNA was established, and no morphological change was observed (data not shown), indicating that all transfected siRNAs show no off-target inhibition to host gene and no cytotoxicity to FHM cells.

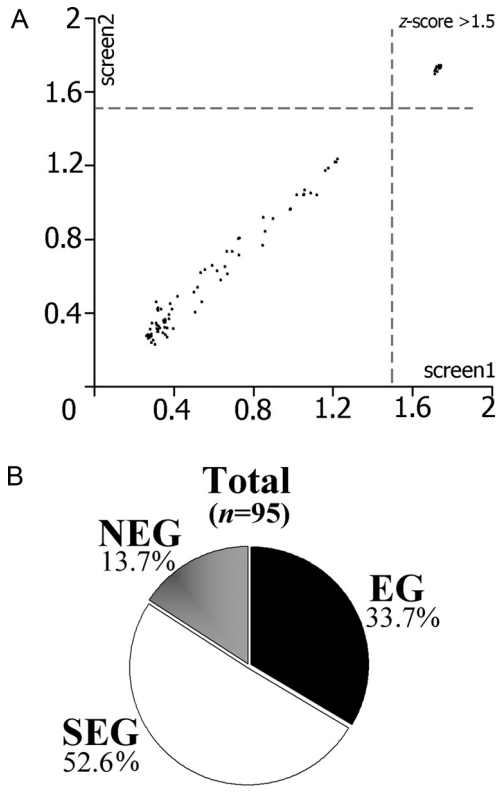

Fig. 2. Genome-wide RNAi screens of TFV. (A) Scatter plot of two genome-wide RNAi screens. Correlation coefficient of *z* scores from duplicate screens was 0.99. Gray broken lines demarcate ORFs classified with a *z* score of three standard deviations or above determined as mEGs. (B) Pie chart of three types of TFV ORFs. Ninety-five TFV ORFs were classified into three groups by *z* score. The quantities and ratios of three types of ORFs were shown.

Furthermore, representative IE, DE, and L ORFs were selected to detect the expression in different siRNA-transfected samples and to verify the specificity of RNAi assays. Selecting appropriate time points for detection is crucial because some non-targeted viral genes are also affected in the cascade of viral gene expression when an important gene is silenced. That is, RNAi silencing of a functionally important viral gene hampers viral replication. In addition, longer monitoring period of life cycle means more severe inhibition of viral replication. To eliminate such a disturbance, the early stage of replication is normally selected (Sample et al., 2007). In the early stage, some genes are not expressed or undetectable. Hence, the right time point should be set as early as possible for easy detection. In the present study, a very early stage of TFV replication, 12 hpi, was selected to detect RNAi specificity for the IE (ORF087R and ORF097R) and L (ORF096R) genes. For the DE genes (ORF016R and ORF022R), 36 hpi was selected. As shown in Fig. S2, the expression levels of these five selected ORFs were analyzed using Sq-RTPCR under five siRNA-transfected conditions. All siRNAs silenced the corresponding ORFs efficiently without severely inhibiting other ORFs. However, the overall expression of the other ORFs was reduced by a certain highly efficient siRNA. A similar effect was also reported in other RNAi experiments against ranavirus (Sample et al., 2007). The expression reduction of the non-targeted ORFs can be attributed to the gene expression cascade in the viral replication mentioned above but not to the off-target effect. The important functions of the IE EG ORF087R and ORF097R were restrained in the early stage of viral replication, which inhibited the expression of DE and L ORFs. The cross effects of ORF087R and ORF097R were also observed in comparison with the si087 or si097 and MT samples. For DE, the inhibition of ORF016R or ORF022R induced the cross effects. However, their inhibition did not reduce IE expression and induce a small decrease in L expression. Silencing of ORF096R, the *mcp* gene, did not change DE expression and slightly reduced IE expression. Similar results were reported by previous study (Xie et al., 2005). Consequently, the specificity of RNAi assay was confirmed, even if some complicated expression situations were present. Such situations were probably due to the expression linkages of viral genes. The abovementioned results may show the gene expression cascade and modulation model in TFV proliferation. Therefore, the IE genes are important throughout TFV life cycle, and IE silencing reduces the robust expression of the IE, DE, and L genes, resulting in great inhibition of viral proliferation. Hence, the IE EGs may be valuable targets for anti-TFV study.

3.3. Validation of RNAi screening by quantitative RT-PCR and titer assay on selected TFV genes

Genome-wide RNAi screening against TFV was performed based on the severity and the emergence time of CPE. Q-CPE assay offered

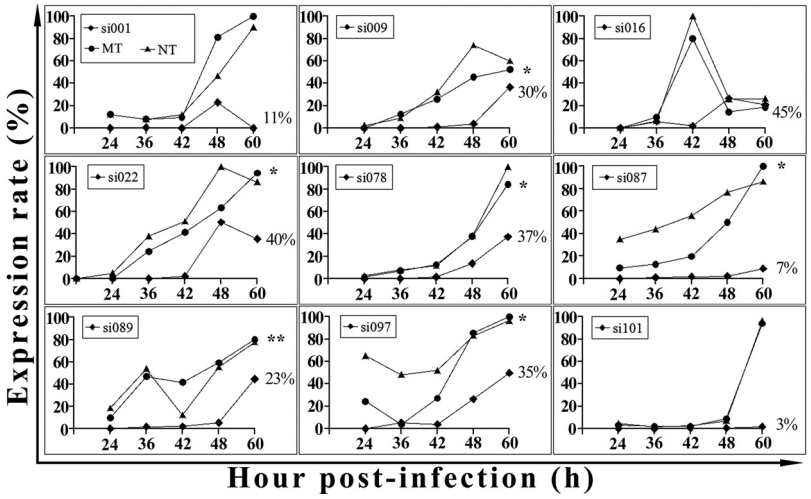

Fig. 3. Expression rate of selected ORFs in RNAi assay. Nine ORFs were selected to perform Sq-RTPCR to determine the expression rate (%) in conditions of siRNA transfected, mock-transfected (MT) or no treatment (NT) at five time intervals post TFV infection. 18S rRNA gene was served as internal control. The electrophoresis images are shown in Fig. S1. Each percentage at the right of the trend line is the average expression rate of siRNA transfected sample to that of the MT sample. The asterisks represent that the expression of siRNA transfected sample was significantly lower than that of MT control (*$p < 0.05$).

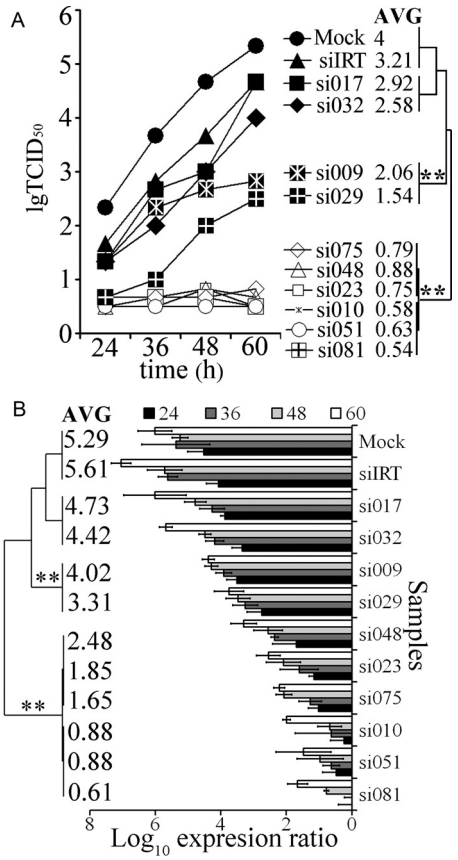

Fig. 4. Quantitative RT-PCR (Q-RTPCR) and titer assays of selected ORFs in RNAi assay. (A) Titer assays of ten selected TFV ORFs. Including mock-transfection (MT) and irrelevant siRNAs control (siIRT), titers of four time points post infection were tested. The average titer (AVG) of all time points of each sample is shown on right and grouped ($p < 0.01$) by hierarchical clustering (Cluster 3.0). (B) Q-RTPCR assays of ten selected TFV ORFs. Q-RTPCR was performed to detect the expression of *mcp* gene in four time intervals after RNAi and FHM 18S rRNA was served as internal control. The average expression ratio (AVG) of all time points of each sample is shown on left and grouped ($p < 0.01$) by hierarchical clustering. Both in Q-RTPCR and titer assays, the selected ORFs were clustered into three groups that were identical to their grouped results of Q-CPE.

the basis information of TFV proliferation. Thus, the changes in each TFV protein were not determined using the protein quantitative method. In addition, some protein factors cannot be easily detected because of low protein levels. Therefore, we selected 10 TFV genes for TFV quantification with more accurate methods, including titer assay and Q-RTPCR, to further confirm the feasibility and credibility of the screening and scaling systems. The 10 selected genes were ORFs, 009L, 010R, 017R, 023R, 029R, 032R, 048L, 051L, 075R, and 081R. The siIRT and MT samples were also included as controls. FHM cells were transfected with corresponding siRNAs and then infected with TFV. At 24, 36, 48, and 60 hpi, the supernatants were collected for titer assay and cells were lysed for RNA extraction followed by Q-RTPCR assay.

Titer assay, which can directly show the quantity of infectious virus, is more precise than other detection methods based on nucleic acids or proteins for evaluating the viral proliferation level. If a given gene is actively involved in the viral proliferation, the titer of a corresponding sample in RNAi assay will markedly decline in siRNA treatment. To inspect the viral quantities in different targeting samples after RNAi, the supernatants of infected cell samples at 24, 36, 48, and 60 hpi were collected for titer assays. The data of titer assays are shown in Table S5. As shown in the graphical chart of Fig. 4A, 12 trend lines representing 12 samples, including MT and siIRT control samples, were used to plot the time-course titer variation. As shown in the right part of Fig. 4A, 12 trend lines were clearly classified into three groups that were further verified by the clustering of each sample's average titer from four time intervals. In the control set comprising MT and siIRT samples, the average titer was 3.6 $lgTCID_{50}\ ml^{-1}$. The average titers in the group I (0.695 $lgTCID_{50}\ ml^{-1}$) and II (1.8 $lgTCID_{50}\ ml^{-1}$) samples targeting six ORFs (081R, 051L, 010R, 075R, 023R, and 048L) and two ORFs (009L and 029R) were 794 ($10^{2.9}$) and 63 ($10^{1.8}$) times lower than that in control set, respectively ($p < 0.01$). These two groups of samples were classified as EGs and SEGs, respectively. The average titer in group III (2.75 $lgTCID_{50}\ ml^{-1}$) samples targeting ORFs 017R and 032R was lower than that in the control set. These samples were classified as NEGs. The rank of the average titer of the selected ORFs was nearly identical to that in the Q-CPE assay (Table 1), verifying that the Q-CPE scaling system worked well in RNAi screening.

On the level of RNA transcripts, Q-RTPCR assay is among the most sensitive and reliable methods for determining the level of RNA transcripts. The *mcp* gene is a valuable detection marker for the infection and quantification of iridovirus (Chinchar, 2002). The transcriptional level of *mcp* can reflect the quantity and proliferation condition of TFV. Thus, Q-RTPCR was performed to detect the transcribed RNA of the *mcp* gene and to monitor the changes of TFV quantity after RNAi. At each time interval, the expression levels of *mcp* were normalized to that of FHM 18S rRNA, and relative expression ratios were generated (Table S6). As shown in Fig. 4B, the positions of all samples on the *x* axis were arranged in an increasing manner by the average *mcp* expression level at 24, 36, 48, and 60 hpi. The *mcp* expression of the siIRT samples was robust and similar to that of the MT samples. The RNAi inhibition of ORFs, 081R, 051L, 010R, 075R, 023R, and 048L suppressed *mcp* expression efficiently, indicating the interference in TFV proliferation. The average *mcp* expression levels at four time intervals for all samples were applied to hierarchical clustering program and were evidently classified into three groups (left part of Fig. 4B). Group I (EGs) ORFs, 010R, 023R, 048L, 051L, 075R, and 081R represented the best result of RNAi assay of 10 selected genes. The average *mcp* expression level of these six samples was 25 ($10^{1.39}$) copies/cell. By contrast, 4677 ($10^{3.67}$) and 38,019 ($10^{4.58}$) copies/cell were the average *mcp* expression levels obtained for group II samples (SEGs, ORF009L and ORF029R) and group III (NEGs, ORF017R and ORF032R) samples, respectively. The average *mcp* expression level of the control sets ($10^{5.45}$ copies/cell), including MT and siIRT samples, was 11,481 ($10^{4.06}$) times higher than that of group I ($p < 0.01$). Consequently, the rank of the expression ratios of the selected ORFs was nearly identical to that in the Q-CPE assay, further verifying that the Q-CPE scaling system can be used in RNAi screening.

High-throughput and large-scale RNAi screening for determining viral proliferation-important genes is indispensable for gene functional research. A reliable and appropriate detection method guarantees the accuracy of the screens. In this study, we used Q-CPE to determine the proliferation level of TFV in the RNAi screens of functionally important genes. The efficiency and specificity of RNAi against TFV were confirmed to meet the demands in the screening by Sq-RTPCR. The Q-CPE results were verified by Q-RTPCR and titer assay even with slight differences in ranking which can be attributed to the incomprehensive single detection factor used by these two methods. Nevertheless, the slight differences from different detection methods were within the margin of error. The consistent results from Q-CPE, titer assay, and Q-RTPCR, indicate that the screening and scaling system for TFV proliferation-important genes by RNAi is feasible and credible.

3.4. TFV EGs

When the most abundant domain predictions were used to categorize genes into distinct functional classes (Eaton et al., 2007;

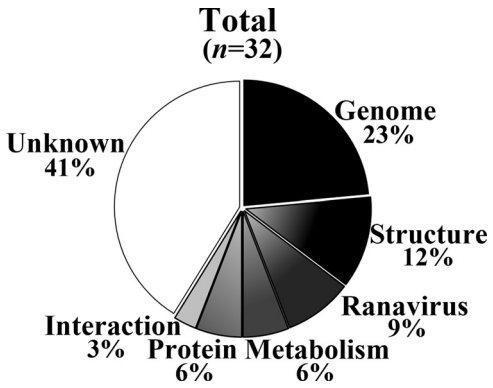

Fig. 5. Representative categories and their percentages of EGs. According to the identifiable proteins or domains, eighteen EGs were classified into six groups including genome-associated factors (Genome), structure proteins and virion morphogenesis-associated proteins (Structure), well-known ranavirus-specific proteins (*Ranavirus*), nucleotide metabolism-related proteins (Metabolism), protein modifications-related proteins (Protein) and host–virus interaction related protein (Interaction). The rest fourteen EGs were grouped as uncharacterized genes (Unknown).

Yutin et al., 2009), the relative distribution of predicted gene functions differed with the quantitative severity of the RNAi phenotypes. Among the 32 EGs, 18 were identified or predicted to encode identifiable protein domains and 14 were uncharacterized genes (41% of EGs) requiring intensive research (Fig. 5). As indicated in Table 1, 18 characterized TFV EGs encode (i) well-known ranavirus-specific proteins (9%), ORF025R (p31K-like protein), ORF087R (ICP-18), and ORF097R (ICP-46); (ii) genome-associated factors (DNA replication, recombination and repair, 23%), ORF009L (Helicase), ORF022R (D5 family ATPase), ORF051L (after SAF-A/B, Acinus and PIAS, SAP DNA-binding protein), ORF065L (DdRP II), ORF089R (DMet), and ORF101R (RAD2); (iii) protein modification-related proteins (6%), ORF029R (Tyrosine protein kinase) and ORF084R (ATPase-dependent protease); (iv) nucleotide metabolism-related proteins (6%), ORF041R (RDRA) and ORF088R (TS); (v) host–virus interaction-related protein (3%), ORF104R (MCL), which is probably an apoptosis regulator protein; (vi) structural proteins and virion morphogenesis-associated proteins (12%), ORF001L (Envelope protein), ORF020R (Envelope protein), ORF048L (NTH1), and ORF096R (MCP). The ratios of these six groups are shown in Fig. 5. Obviously, EGs cover many types of genes, the two most populated categories of which are the factors (25%) of DNA replication, recombination, and repair, and proteins (12.5%) of virion structure and morphogenesis. To further narrow the range of EG, we selected 16 cases in which siRNA resulted in TFV proliferation inhibition of as shown by a *z* score of 1.5 or higher. This threshold included RNAi phenotypes ranging in severity from *z* scores of 1.70–1.74. These phenotypes represent the most important EG (mEG) in TFV proliferation cycle. The rank of *z* scores of TFV ORFs are shown in Table S3. RNAi technology allows a more rapid and convenient identification of EGs and NEGs than the traditional method such as direct random mini-transposon mutagenesis (Brune et al., 1999).

The directional and constructive evidences of genome-wide RNAi are crucial to select significant viral ORFs for further functional research. For example, the TFV mEGs ORF087R and ORF097R are homologous to the well-known FV3 IE proteins, ICP-18 (18K, encoded by ORF82R) and ICP-46 (46K, encoded by ORF91R) (Beckman et al., 1988; Xia et al., 2010), that are closely related to viral regulation in the early stage of infection (Xia et al., 2009). However, our results on ORF087R are different from the inhibition study of FV3 18K IE protein (ORF82R), which was determined nonessential for FV3 replication in FHM cells using antisense morpholino oligonucleotide (Sample et al., 2007). On the other hand, the importance of TFV ORF097R was verified by a homology study on FV3 ORF91R (Whitley et al., 2011). The discrepancy in two very similar viruses that may represent strains of the same viral species has yet to be clarified (Chinchar et al., 2005). TFV ORF025R is also a mEG of TFV. ORF025R is homologous with the FV3 essential protein (P31K, encoded by ORF91R) which is ranavirus-specific protein involving in the passage from the nuclear to the cytoplasmic phase of viral DNA replication (Martin et al., 1984).

Six EGs are the factors responsible for TFV DNA replication, recombination, and repair. ORF022R (D5 ATPase) may play an important role prior to viral genome replication (Chen et al., 2006). ORF065L (DdRP II), the viral homolog of the largest subunit of RNA polymerase II, may be responsible for the late gene expression of ranavirus and may greatly affect virus yields (Sample et al., 2007). Our results support these hypotheses. ORF009L (a predicted helicase) and ORF022R (D5 family ATPase) are predicted to involve various processes including transcription regulation, DNA repair, DNA recombination, and chromatin unwinding (Laurent et al., 1991). A SAP DNA-binding domain is encoded by TFV ORF051L, suggesting that ORF051L is involved in chromosomal organization. ORF089R (DMet) may play a crucial role in the expression of the viral genome (Willis and Granoff, 1980) by viral genomic methylation (Kaur et al., 1995). ORF101R (RAD2) functions in the nucleotide excision repair and transcription coupled repair of oxidative DNA damage (Tan et al., 2004). The importance of the DMet gene in iridovirus was previously proven by RNAi in FV3-FHM infection model (Whitley et al., 2011).

The potential factors involved in protein modifications are ORF029R (Tyrosine protein kinase) and ORF084R (ATPase-dependent protease) that function in posttranslational modification, protein turnover, and chaperone activity (Ramachandran et al., 2002). The EGs involved in TFV nucleotide metabolism include ORF088R (TS), which is the most conserved protein in the TFV genome from bacteria to human, and ORF041R (RDRA), which is the α subunit of ribonucleoside-diphosphate reductase commonly found in numerous cytoplasmic DNA viruses (He et al., 2002). However, ORF071L (RDRB), the β subunit of ribonucleoside-diphosphate reductase, was characterized as an SEG. These findings suggest that α and β subunits, ORF041R and ORF071L, are not functionally equalized in TFV life cycle. In addition to the essential proteins that are required for viral replication, TFV also encodes putative factors involved in host–virus interaction, such as ORF104R (MCL), which is a Bcl-2-like protein that possibly manipulates the balance of life and death in TFV infected cells and regulates cell apoptosis, corroborating previous findings that several iridovirus agents can induce apoptosis during infection (Chinchar et al., 2003; Huang et al., 2007).

Structural proteins are obviously essential to the life cycle of TFV. As shown in Table 1, ORF096R (*mcp*) was characterized as EG but was not the mEG. However, ORF096R scored the highest among the EGs, and the *mcp* gene of ranavirus is essential for infectious virus production as previously demonstrated (Sample et al., 2007; Xie et al., 2005). Aside from the capsid protein, two verified viral membrane (envelope) proteins, ORF001L and ORF020R (Wang et al., 2008), were also characterized as mEGs required for TFV proliferation. ORF048L is a virion morphogenesis associated mEG that encodes NTH1, the major cytoskeletal structure of many neurons (Soppet et al., 1992). ORF048L may contribute to the release of viral particles from infected cells or to the intracellular trafficking. Nevertheless, another highly relative NTH1 which may be a virion protein (Kim et al., 2010; Zhao et al., 2008), ORF033R, was defined as SEG. A homologous gene in FV3 (ORF32R) was verified essential for FV3 proliferation and extensive works are undergoing (Whitley et al., 2011). Overall, these results indicate that the virion structure or morphogenesis-associated proteins are important for TFV

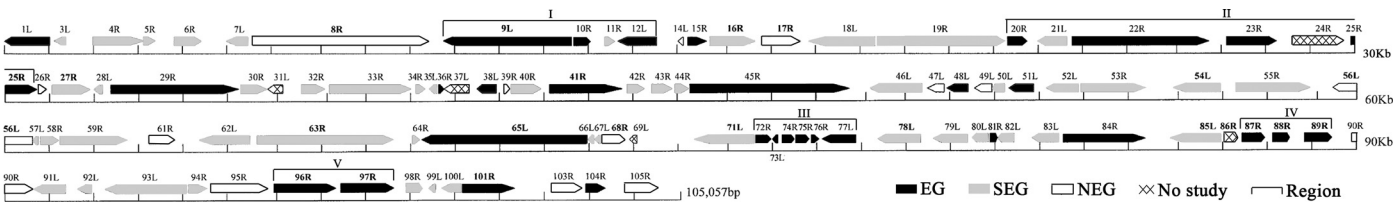

Fig. 6. TFV genome map with ORFs organization of proliferation importance. Arrows represent TFV ORFs, indicating the location, orientation, and putative size. Black, gray and white arrows represent EGs, SEGs and NEGs respectively. Crosses indicate non-study ORFs and frames show the discrete regions of tandem EGs.

propagation and may be potential targets for antiviral research and vaccine development.

3.5. Distribution of EGs in TFV genome

To clearly delineate the important regions in TFV genome, we marked all the screened genes on a linear physical map of TFV in correlation with updated genome sequence data (He et al., 2002) (Fig. 6). The relationship between the physical location and the importance of a given ORF is illustrated in the figure. For most of the EGs, cluster distribution was found in the genome. As numbered in black frames, at least five discrete regions of tandem EGs (from I to V) were present. Important factors or enzymes were in regions II and IV, suggesting that the genes in these regions may be regulated or transcribed synchronously to facilitate the response to the external environment or stimulation (Chinchar, 2002). In addition, six EGs (ORFs, 072R, 073L, 074R, 075R, 076R, and 077L) in region III were not homologous to any conserved domain or signature in the family *Iridoviridae*, indicating that this functionally unknown region is a valuable target for antiviral research and recombinant virus study. Moreover, the ORF prediction of region III in TFV is more precise than that in FV3 and *Ambystoma tigrinum virus* (ATV) (Eaton et al., 2007). However, the genes of structural proteins, such as ORFs, 001L, 020R, 048L, and 096R, are scattered in the genome for robust transcription in the late stage of viral replication, preventing the interference of each other (Chinchar et al., 2005). The distribution study may reveal the network of relationships between viral ORFs in proliferation, which requires further study of viral functional genomics. Proliferation-related EGs are the potential targets for therapeutic research.

3.6. Comparative analysis of the EGs in Ranavirus

In the family *Iridoviridae* genus *Ranavirus*, the genome sequence and ORF annotation of TFV are markedly similar to those of ATV, soft-shelled turtle iridovirus (STIV), and FV3, the type species of this genus. Therefore, a comparative analysis between TFV and FV3/ATV/STIV will benefit the gene functional research of ranaviruses. TFV EGs were screened by genome-wide RNAi and EGs are relatively conservative in sequence along with the viral evolution because of the important gene function. More than 78% of TFV EGs shared high similarity to corresponding homologs in ranaviruses (FV3/ATV/STIV). However, ORFs, 036R, 038L, 072R, 073L, 075R, 077R, and 088R possessed homologs only in one or two ranaviruses, as shown in Table 2. ORFs, 036R, 038L, and 075R possessed no homologs in ATV and ORFs, 038L, 072R, 073L, 075R, 077L, and 088R possessed no homologs in STIV. This result suggests that ATV/STIV should be re-annotated to the corresponding ORFs, especially the STIV genome regions ranging from 78,236 to 80,316. ORF038L, a functionally characterized ORF, had a homolog in FV3, *Rana grylio* iridovirus (AFG73081), *Andrias davidianus* ranavirus (AHA42342), and Chinese giant salamander iridovirus (AHA80921) but not in ATV and STIV, implying that the analogous genome regions of ranaviruses should be studied intensively. Interestingly, the structural protein ORF048L showing only approximately 70% identity with FV3/ATV/STIV, is probably the determining factor of structural difference with these closely related ranaviruses. ORF087R (ICP-18) showed approximately 89% identity with the counterpart of the FV3 18K protein. The low homology of these two proteins may be the reason why the 18K protein is not essential for FV3 replication in FHM (Sample et al., 2007) and in vivo (Chen et al., 2011). ORF088R, a viral essential thymidylate synthase that showed 72% identity with herpes virus (AAL14421), had homologous ORFs in ATV but not in FV3 and STIV. The region from ORFs 072R to 077L of TFV should be studied intensively because of the clustering of TFV EGs in this region and the different annotations between ranaviruses (Eaton et al., 2007).

Table 2
Comparative analysis of TFV EGs with FV3, ATV and SGIV.

ORF No.	Predicted structure or function	Identity (%)[a]		
		FV3	STIV	ATV
001L	Envelope protein	98	98	97
009L	Helicase	98	98	97
010R		99	99	99
012L		98	99	97
015R		99	99	96
020R	Envelope protein	90	96	88
022R	D5 family ATPase	98	99	97
023R		96	97	92
025R	p31K-like protein	99	99	97
029R	Tyrosine protein kinase	97	98	95
036R		97	98	–
038L		47	–	–
041R	Ribonucleoside-diphosphate reductase α (RDRA) chain	98	98	97
045R		98	98	96
048L	Neurofilament triplet H1-like protein (NTH1)	71	69	61–70
051L	SAP DNA-binding protein	98	98	94
065L	DNA-directed RNA polymerase II (DdRPII) second largest subunit	98	98	96
072R		90	–	88
073L		–	–	80
074R		99	99	97
075R		98	–	–
076R		96	95	91
077L		96	–	95
081R		95	96	96
084R	ATPase-dependent protease	97	97	86
087R	Immediate early protein (ICP-18)	89	89	94
088R	Thymidylate synthase (TS)	–	–	95
089R	Cytosine DNA methyltransferase (DMet)	96	96	96
096R	Major capsid protein (MCP)	98	99	96
097R	Immediate early protein (ICP-46)	96	97	94
101R	DNA repair protein RAD2	98	98	97
104R	Myeloid cell leukemia protein (MCL)	93	94	85

– denotes no blast result.
[a] Percentage of amino acid identity based on BLASTP analysis.

3.7. SEGs and NEGs of TFV

Fifty ORFs were determined as SEGs in the screens. Differences in the importance of the SEGs can be predicted although more than 50% of TFV ORFs were classified into this category. In addition, the viral EGs for in vivo propagation may not have the same role or equally important function as the SEGs for replication in a cultural cell line in vitro. For example, the viral encoded eIF-2α-like protein (vIF-2α) in FV3, a homolog of TFV ORF027R, is necessary for viral replication and growth in vivo (Chen et al., 2011), whereas the vIF-2α protein in BIV is not essential for viral replication in vitro (Pallister et al., 2007). The functions of both proteins were verified by gene-defective recombinant virus. The vIF-2α protein is involved in the initiation (Antoun et al., 2003) and maintenance of translation by mimicking the host eIF-2α to prevent PKR (dsRNA-activated protein kinase)-mediated phosphorylation (Chinchar, 2002; Rothenburg et al., 2011) or to degrade fish PKZ (protein kinase containing Z-DNA binding domains) (Jancovich and Jacobs, 2011), resulting in the innate immune evasion of ranaviruses. Therefore, TFV ORF027R is a SEG in vitro and possibly a virulence gene for TFV growth in vivo.

Aside from MCP, a predicted myristoylated membrane protein (ORF055R) encoded by TFV, is a structural protein that may be important in viral replication. The homolog of this protein in FV3 (ORF53R) is essential for viral replication when the FV3 titer drops to less than 40% of the wild type virus, as prove by RNAi (Whitley et al., 2010). Moreover, the homologous protein (53R) in *Rana grylio* virus (RGV) was also proven important by an artificial microRNA method, the results of which were verified by 6- to 17-fold drop in virus titer under silencing condition (Kim et al., 2010). In TFV RNAi screens, ORF055R was determined as a SEG in group II whose the average titer was approximately 10-fold lower than that of the control set in the titer assay of the selected genes above. These results indicate that the myristoylated membrane proteins of ranavirus are valuable targets for vaccine development.

Surprisingly, 13 TFV ORFs were characterized as NEGs, including 5 ORFs with identifiable protein products that mainly contain the enzymes (Table 1). These 5 ORFs include (i) the nucleotide metabolism-associated enzyme ORF068R (dUTPase); (ii) the host–virus interaction factor ORF090R (PCNA); and (iii) the DNA replication, repair, and modification enzymes ORF017R (Integrase), ORF056L (Helicase-like protein), and ORF105R (RF). These enzymes may be unnecessary in viral replication or substituted by other enzymes or pathways under RNAi conditions. However, nuclear cytoplasmic large DNA viruses from the families *Iridoviridae*, *Poxviridae*, *Asfarviridae*, *Ascoviridae*, *Phycodnaviridae*, *Mimiviridae*, and the proposed family "*Marseilleviridae*" (Colson et al., 2013) showed that some genes are "useless" in in vitro propagation or in specific cell lines but are essential for multiplying in vivo (Filée, 2013). Therefore, the screened NEGs of TFV in this study were the results of the TFV-FHM infection model. The propagation details of TFV in different cell lines, especially human cell line, should be studied further because TFV is a powerful virus that can infect various types of cell lines. Nevertheless, the inevitable drawbacks of siRNA-mediated RNAi might have caused the high ratio of NEGs. Other methods that can overcome the defect of RNAi should be used to describe the function of a single gene or to precisely screen the importance of genes on a genome-scale. One of these methods is clustered regularly interspaced short palindromic repeats (CRISPR). The RNA-guided CRISPR-associated nuclease Cas9 (CRISPR/Cas9 system) is an improved method for the knockout of individual genes in genome-scale functional screens (Mali et al., 2013). This method can completely disrupt target genes by genome editing, thereby avoiding weak signals that can occur when transcript abundance is partially decreased by siRNA. Furthermore, gene targeting by the CRISPR system is more precise and may produce substantially fewer off-target effects than existing methods (Barrangou, 2013). Wang et al. (2014) and Shalem et al. (2014) used the powerful bacterial CRISPR/Cas9 system with protocols that avoid the pitfalls associated with siRNA to screen the important genes in human cell lines both in negative and positive selections.

In sum, the genome-scale results of RNAi assay in this study may provide insights into viral replication and pathogenesis strategies, and may also be valuable to research on iridovirus.

Acknowledgements

This research was supported by The National High Technology Research and Development Program of China (863 Program) (No. 2012AA10A407); The National Natural Science Foundation of China (No. 31370048); The National Basic Research Program of China (973 program) (No. 2012CB114406); Guangdong Natural Science Foundation (2011A020102002).

Appendix A. Supplementary data

Supplementary data associated with this article can be found, in the online version, at http://dx.doi.org/10.1016/j.virusres.2014.05.020.

References

Abdulnaser, A., Sarah, S., John, H., Peter, J., Sofi, I., 2009. Inhibition of Monkeypox virus replication by RNA interference. Virol. J. 6, 188.
Andino, R., 2003. RNAi puts a lid on virus replication. Nat. Biotechnol. 21, 629–630.
Antoun, A., Pavlov, M.Y., Andersson, K., Tenson, T., Ehrenberg, M., 2003. The roles of initiation factor 2 and guanosine triphosphate in initiation of protein synthesis. EMBO J. 22, 5593–5601.
Ashrafi, K., Chang, F.Y., Watts, J.L., Fraser, A.G., Kamath, R.S., Ahringer, J., Ruvkun, G., 2003. Genome-wide RNAi analysis of *Caenorhabditis elegans* fat regulatory genes. Nature 421, 268–272.
Barrangou, R., 2013. CRISPR-Cas systems and RNA-guided interference. Wiley Interdiscip. Rev. RNA 4, 267–278.
Beckman, W., Tham, T.N., Aubertin, A.M., Willis, D.B., 1988. Structure and regulation of the immediate-early frog virus 3 gene that encodes ICR489. J. Virol. 62, 1271–1277.
Bettencourt-Dias, M., Giet, R., Sinka, R., Mazumdar, A., Lock, W.G., Balloux, F., Zafiropoulos, P.J., Yamaguchi, S., Winter, S., Carthew, R.W., Cooper, M., Jones, D., Frenz, L., Glover, D.M., 2004. Genome-wide survey of protein kinases required for cell cycle progression. Nature 432, 980–987.
Boutros, M., Kiger, A.A., Armknecht, S., Kerr, K., Hild, M., Koch, B., Haas, S.A., Consortium, H.F., Paro, R., Perrimon, N., 2004. Genome-wide RNAi analysis of growth and viability in Drosophila cells. Science 303, 832–835.
Brune, W., Menard, C., Hobom, U., Odenbreit, S., Messerle, M., Koszinowski, U.H., 1999. Rapid identification of essential and nonessential herpesvirus genes by direct transposon mutagenesis. Nat. Biotechnol. 17, 360–364.
Chen, G., Ward, B.M., Yu, K.H., Chinchar, V.G., Robert, J., 2011. Improved knockout methodology reveals that frog virus 3 mutants lacking either the 18K immediate-early gene or the truncated vIF-2alpha gene are defective for replication and growth in vivo. J. Virol. 85, 11131–11138.
Chen, L.M., Wang, F., Song, W.J., Hew, C.L., 2006. Temporal and differential gene expression of Singapore grouper iridovirus. J. Gen. Virol. 87, 2907–2915.
Chinchar, V.G., 2002. Ranaviruses (family *Iridoviridae*): emerging cold-blooded killers. Arch. Virol. 147, 447–470.
Chinchar, V.G., Bryan, L., Wang, J., Long, S., Chinchar, G.D., 2003. Induction of apoptosis in frog virus 3-infected cells. Virology 306, 303–312.
Chinchar, V.G., Essbauer, S., He, J.G., Hyatt, A., Miyazaki, T., Seligy, V., Williams, T., 2005. Part II the double stranded DNAviruses, family Iridoviridae. In: Fauquet, C.M., Mayo, M.A., Maniloff, J., Desselberger, U., Ball, L.A. (Eds.), Virus Taxonomy, VIIIth Report of the International Committee on Taxonomy of Viruses. Elsevier/Academic Press, London, pp. 145–162.
Colson, P., De Lamballerie, X., Yutin, N., Asgari, S., Bigot, Y., Bideshi, D.K., Cheng, X.W., Federici, B.A., Van Etten, J.L., Koonin, E.V., La Scola, B., Raoult, D., 2013. "Megavirales", a proposed new order for eukaryotic nucleocytoplasmic large DNA viruses. Arch. Virol. 158, 2517–2521.
Crouch, S.P., Kozlowski, R., Slater, K.J., Fletcher, J., 1993. The use of ATP bioluminescence as a measure of cell proliferation and cytotoxicity. J. Immunol. Methods 160, 81–88.
Eaton, H.E., Metcalf, J., Penny, E., Tcherepanov, V., Upton, C., Brunetti, C.R., 2007. Comparative genomic analysis of the family *Iridoviridae*: re-annotating and defining the core set of iridovirus genes. Virol. J. 4, 11.
Elbashir, S.M., Harborth, J., Lendeckel, W., Yalcin, A., Weber, K., Tuschl, T., 2001. Duplexes of 21-nucleotide RNAs mediate RNA interference in cultured mammalian cells. Nature 411, 494–498.

Filée, J., 2013. Route of NCLDV evolution: the genomic accordion. Curr. Opin. Virol. 3, 595–599.
Fire, A., Xu, S., Montgomery, M.K., Kostas, S.A., Driver, S.E., Mello, C.C., 1998. Potent and specific genetic interference by double-stranded RNA in *Caenorhabditis elegans*. Nature 391, 806–811.
Fjose, A., Ellingsen, S., Wargelius, A., Seo, H.C., 2001. RNA interference: mechanisms and applications. Biotechnol. Annu. Rev. 7, 31–57.
Fraser, A.G., Kamath, R.S., Zipperlen, P., Martinez-Campos, M., Sohrmann, M., Ahringer, J., 2000. Functional genomic analysis of *C. elegans* chromosome I by systematic RNA interference. Nature 408, 325–330.
Gönczy, P., Echeverri, C., Oegema, K., Coulson, A., Jones, S.J., Copley, R.R., Duperon, J., Oegema, J., Brehm, M., Cassin, E., Hannak, E., Kirkham, M., Pichler, S., Flohrs, K., Goessen, A., Leidel, S., Alleaume, A.M., Martin, C., Ozlü, N., Bork, P., Hyman, A.A., 2000. Functional genomic analysis of cell division in *C. elegans* using RNAi of genes on chromosome III. Nature 408, 331–336.
Hamilton, M.A., Russo, R.C., Thurston, R.V., 1977. Trimmed Spearman–Karber method for estimating median lethal concentrations in toxicity bioassays. Environ. Sci. Technol. 11, 714–719 (correction 1978, 12, 417).
He, J.G., Lü, L., Deng, M., He, H.H., Weng, S.P., Wang, X.H., Zhou, S.Y., Long, Q.X., Wang, X.Z., Chan, S.M., 2002. Sequence analysis of the complete genome of an Iridovirus isolated from the Tiger Frog. Virology 292, 185–197.
Hsuana, S.L., Changa, S.C., Wangb, S.Y., Liaoa, T.L., Jongc, T.T., Chiena, M.S., Leea, W.C., Chend, S.S., Liao, J.W., 2009. The cytotoxicity to leukemia cells and antiviral effects of Isatis indigotica extracts on pseudorabies virus. J. Ethnopharmacol. 123, 61–67.
Huang, Y.H., Huang, X.H., Gui, J.F., Zhang, Q.Y., 2007. Mitochondrion-mediated apoptosis induced by *Rana grylio* virus infection in fish cells. Apoptosis 12, 1569–1577.
Iyer, L.M., Aravind, L., Koonin, E.V., 2001. Common origin of four diverse families of large eukaryotic DNA viruses. J. Virol. 75, 11720–11734.
Iyer, L.M., Balaji, S., Koonin, E.V., Aravind, L., 2006. Evolutionary genomics of nucleocytoplasmic large DNA viruses. Virus Res. 117, 156–184.
Jancovich, J.K., Jacobs, B.L., 2011. Innate immune evasion mediated by the *Ambystoma tigrinum* virus eukaryotic translation initiation factor 2alpha homologue. J. Virol. 85, 5061–5069.
Kamath, R.S., Fraser, A.G., Dong, Y., Poulin, G., Durbin, R., Gotta, M., Kanapin, A., Le Bot, N., Moreno, S., Sohrmann, M., Welchman, D.P., Zipperlen, P., Ahringer, J., 2003. Systematic functional analysis of the *Caenorhabditis elegans* genome using RNAi. Nature 421, 231–237.
Kaur, K., Rohozinski, J., Goorha, R., 1995. Identification and characterization of the frog virus 3 DNA methyltransferase gene. J. Gen. Virol. 76, 1937–1943.
Kim, Y.S., Ke, F., Lei, X.Y., Zhu, R., Zhang, Q.Y., 2010. Viral envelope protein 53R gene highly specific silencing and iridovirus resistance in fish Cells by AmiRNA. PLoS ONE 5, e10308.
Laurent, B.C., Treitel, M.A., Carlson, M., 1991. Functional interdependence of the yeast SNF2, SNF5, and SNF6 proteins in transcriptional activation. Proc. Natl. Acad. Sci. U.S.A. 88, 2687–2691.
Liu, W., Saint, D.A., 2002. A new quantitative method of real time reverse transcription polymerase chain reaction assay based on simulation of polymerase chain reaction kinetics. Anal. Biochem. 302, 52–59.
Liu, Y., Yang, Z., He, J., Shi, L., Xiao, H., 2005. Comparison and analysis of CPE assay, MTT assay and plaque reductive assay for evaluating medicines in antiviral effects in vitro. Med. J. Wuhan Univ. 26, 199–202.
Lum, L., Yao, S., Mozer, B., Rovescalli, A., Kessler, D.V., Nirenberg, M., Beachy, P.A., 2003. Identification of hedgehog pathway components by RNAi in Drosophila cultured cells. Science 299, 2039–2045.
Luo, Y.W., Weng, S.P., Wang, Q., Shi, X.J., Dong, C.F., Lu, Q.X., Yu, X.Q., He, J.G., 2009. Tiger frog virus can infect zebrafish cells for studying up- or down-regulated genes by proteomics approach. Virus Res. 144, 171–179.
Maeda, I., Kohara, Y., Yamamoto, M., Sugimoto, A., 2001. Large-scale analysis of gene function in *Caenorhabditis elegans* by high-throughput RNAi. Curr. Biol. 11, 171–176.
Mali, P., Yang, L., Esvelt, K.M., Aach, J., Guell, M., DiCarlo, J.E., Norville, J.E., Church, G.M., 2013. RNA-guided human genome engineering via Cas9. Science 339, 823–826.
Martin, J.P., Aubertin, A.M., Tondre, L., Kirn, A., 1984. Fate of frog virus 3 DNA replicated in the nucleus of arginine-deprived CHO cells. J. Gen. Virol. 65, 721–732.
Pallister, J., Goldie, S., Coupar, B., Shiell, B., Michalski, W.P., Siddon, N., Hyatt, A., 2007. Bohle iridovirus as a vector for heterologous gene expression. J. Virol. Methods 146, 419–423.
Petty, R.D., Sutherland, L.A., Hunter, E.M., Cree, I.A., 1995. Comparison of MTT and ATP-based assays for measurement of viable cell number. J. Biolum. Chemilum. 10, 29–34.
Ramachandran, R., Hartmann, C., Song, H.K., Huber, R., Bochtler, M., 2002. Functional interactions of HslV (ClpQ) with the ATPase HslU (ClpY). Proc. Natl. Acad. Sci. U.S.A. 99, 7396–7401.
Ramet, M., Manfruelli, P., Pearson, A., Mathey-Prevot, B., Ezekowitz, R.A., 2002. Functional genomic analysis of phagocytosis and identification of a Drosophila receptor for *E. coli*. Nature 416, 644–648.
Reed, L.J., Muench, H., 1938. A simple method of estimating fifty per cent endpoints. Am. J. Hyg. 27, 493–497.
Rothenburg, S., Chinchar, V.G., Dever, T.E., 2011. Characterization of a ranavirus inhibitor of the antiviral protein kinase PKR. BMC Microbiol. 11, 56.
Sample, R., Bryan, L., Long, S., Majji, S., Hoskins, G., Sinning, A., Olivier, J., Chinchar, V.G., 2007. Inhibition of iridovirus protein synthesis and virus replication by antisense morpholino oligonucleotides targeted to the major capsid protein, the 18 kDa immediate-early protein, and a viral homolog of RNA polymerase II. Virology 358, 311–320.
Schwarz, D., Hutvagner, G., Du, T., Xu, Z., Aronin, N., Zamore, P.D., 2003. Asymmetry in the assembly of the RNAi enzyme complex. Cell 115, 199–208.
Serkedjieva, J., Ivancheva, S., 1999. Antiherpes virus activity of extracts from the medicinal plant *Geranium sanguineum* L. J. Ethnopharmacol. 64, 59–68.
Shalem, O., Sanjana, N.E., Hartenian, E., Shi, X., Scott, D.A., Mikkelsen, T.S., Heckl, D., Ebert, B.L., Root, D.E., Doench, J.G., Zhang, F., 2014. Genome-scale CRISPR-Cas9 knockout screening in human cells. Science 343, 84–87.
Soppet, D.R., Beasley, L.L., Willard, M.B., 1992. Evidence for unequal crossing over in the evolution of neurofilament polypeptide H. J. Biol. Chem. 267, 17354–17361.
Tan, W.G.H., Barkman, T.J., Chinchar, V.G., Essani, K., 2004. Comparative genomic analyses of frog virus 3, type species of the genus *Ranavirus* (family *Iridoviridae*). Virology 323, 70–84.
Tidona, C.A., Schnitzler, P., Kehm, R., Darai, G., 1998. Is the major capsid protein of iridoviruses a suitable target for the study of viral evolution? Virus Genes 16, 59–66.
van den Born, E., Stein, D.A., Iversen, P.L., Snijder, E.J., 2005. Antiviral activity of morpholino oligomers designed to block various aspects of Equine arteritis virus amplification in cell culture. J. Gen. Virol. 86, 3081–3090.
Wang, Q., Luo, Y., Xie, J., Dong, C., Weng, S., Ai, H., Lü, L., Yang, X., Yu, X., He, J., 2008. Identification of two novel membrane proteins from the Tiger frog virus (TFV). Virus Res. 136, 35–42.
Wang, T., Wei, J.J., Sabatini, D.M., Lander, E.S., 2014. Genetic screens in human cells using the CRISPR-Cas9 system. Science 343, 80–84.
Weng, S.P., He, J.G., Wang, X.H., Lü, L., Deng, M., Chan, S.M., 2002. Outbreaks of an iridovirus disease in cultured tiger frog, *Rana tigrina rugulosa*, in southern China. J. Fish Dis. 25, 423–427.
Whitley, D.S., Sample, R.C., Sinning, A.R., Henegar, J., Chinchar, V.G., 2011. Antisense approaches for elucidating ranavirus gene function in an infected fish cell line. Dev. Comp. Immunol. 35, 937–948.
Whitley, D.S., Yu, K., Sample, R.C., Sinning, A., Henegar, J., Norcross, E., Chinchar, V.G., 2010. Frog virus 3 ORF 53R, a putative myristoylated membrane protein, is essential for virus replication in vitro. Virology 405, 448–456.
Willis, D., Granoff, A., 1980. Frog virus 3 DNA is heavily methylated at CpG sequences. Virology 107, 250–257.
Wu, Y., Lü, L., Yang, L.S., Weng, S.P., Chan, S.M., He, J.G., 2007. Inhibition of white spot syndrome virus in *Litopenaeus vannamei* shrimp by sequence-specific siRNA. Aquaculture 271, 21–30.
Xia, L., Cao, J., Huang, X., Qin, Q., 2009. Characterization of Singapore grouper iridovirus (SGIV) ORF086R, a putative homolog of ICP18 involved in cell growth control and virus replication. Arch. Virol. 154, 1409–1416.
Xia, L., Liang, H., Huang, Y., Ou-Yang, Z., Qin, Q., 2010. Identification and characterization of Singapore grouper iridovirus (SGIV) ORF162L, an immediate-early gene involved in cell growth control and viral replication. Virus Res. 147, 30–39.
Xie, J.F., Lü, L., Deng, M., Weng, S.P., Zhu, J.Y., Wu, Y., Gan, L., Chan, S.M., He, J.G., 2005. Inhibition of reporter gene and Iridovirus-tiger frog virus in fish cell by RNA interference. Virology 338, 43–52.
Yutin, N., Wolf, Y.I., Raoult, D., Koonin, E.V., 2009. Eukaryotic large nucleocytoplasmic DNA viruses: clusters of orthologous genes and reconstruction of viral genome evolution. Virol. J. 6, 223.
Zhao, Z., Ke, F., Huang, Y.H., Zhao, J.G., Gui, J.F., Zhang, Q.Y., 2008. Identification and characterization of a novel envelope protein in *Rana grylio* virus. J. Gen. Virol. 89, 1866–1872.